Molecular Insight Into the Hydrogen Bonding and Micro-Segregation of a Cryoprotectant Molecule

ARTICLE *in* THE JOURNAL OF PHYSICAL CHEMISTRY B · OCTOBER 2012

Impact Factor: 3.3 · DOI: 10.1021/jp3093034 · Source: PubMed

3 AUTHORS, INCLUDING:

James Joseph Towey
University of Nottingham
6 PUBLICATIONS **93** CITATIONS
SEE PROFILE

Lorna Dougan
University of Leeds
38 PUBLICATIONS **755** CITATIONS
SEE PROFILE

THE JOURNAL OF PHYSICAL CHEMISTRY B

Article

pubs.acs.org/JPCB

Molecular Insight Into the Hydrogen Bonding and Micro-Segregation of a Cryoprotectant Molecule

J.J. Towey,[†] A.K. Soper,[‡] and L. Dougan[†]

[†]School of Physics and Astronomy, University of Leeds, Leeds, LS2 9JT, United Kingdom

[‡]ISIS Facility, Rutherford Appleton Laboratory, Chilton, Didcot, Oxon, OX11 OQX, United Kingdom

Supporting Information

ABSTRACT: Glycerol–water liquid mixtures are intriguing hydrogen-bonded systems and essential in many fields of chemistry, ranging from basic molecular research to widespread use in industrial and biomedical applications as cryoprotective solutions. Despite much research on these mixtures, the details of their microscopic structure are still not understood. One common notion is that glycerol acts to diminish the hydrogen bonding ability of water, a recurring hypothesis that remains untested by direct experimental approaches. The present work characterizes the structure of glycerol–water mixtures, across the concentration range, using a combination of neutron diffraction experiments and computational modeling. Contrary to previous expectations, we show that the hydrogen bonding ability of water is not diminished in the presence of glycerol. We show that glycerol–water hydrogen bonds effectively take the place of water–water hydrogen bonds, allowing water to maintain its full hydrogen bonding capacity regardless of the quantity of glycerol in the environment. We provide a quantitative measurement of all hydrogen bonding in the system and reveal a concentration range where a microsegregated, bipercolating liquid mixture exists in coexistence with a considerable interface region. This work highlights the role of hydrogen bonding connectivity rather than water structuring/destructuring effects in these important cryoprotective systems.

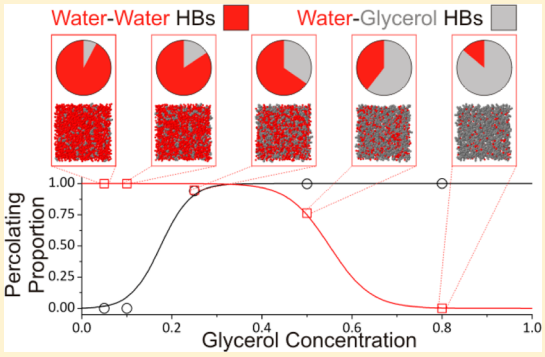

INTRODUCTION

The sugar alcohol glycerol is an intricate, hydrogen-bonding molecule and has been the subject of long-standing scientific interest.[1−3] This attention is partly due to glycerol's ability as a cryoprotectant, acting to stabilize molecules, cells and tissues under cooling to subzero temperatures.[4] Since the pioneering work of Polge et al. in the 1940s,[1] glycerol has become an established molecule of choice in many areas of cryopreservation, revolutionizing areas of biotechnology, plant and animal breeding, the pharmaceutical industry, and modern medicine.[3,5,6] The challenge of successful cryopreservation is the ability to recover as many cells or tissues as possible, after cooling to sub-zero temperatures. A major problem is the changes brought about by the transition of water to ice during cooling, resulting in osmotic stress or "freeze dehydration",[7] as well as physical destruction of membranes by ice and organelle disruption.[8]

While the addition of cryoprotectants, such as glycerol, has become a widespread and almost mundane step within the cryopreservation protocols for many applications, the molecular mechanism of its action remains unclear. This is limiting given that any future advances in cryopreservation rely on developing an understanding of the action of glycerol and having accurate predictive control over cryopreservation protocols.[5] New challenges in biotechnology and in the clinical use of cryopreserved cells or tissues can only be met by moving beyond qualitative descriptions of cryoprotective action.[4,9] Central to this problem is the action of glycerol on the structure of water. Indeed, in the early years of cryopreservation, molecules such as glycerol were called "solute moderators", as they were thought to moderate the structure of water in some way.[10]

In the 1960s, Nash attempted to qualitatively describe this cryoprotectant moderation action based on a combination of parameters including; the ability to modulate hydrogen bonding, interaction with water molecules and the volume occupied by a molecule of the cryoprotectant.[11] However, he recognized that a more comprehensive study of cryoprotection activity was required, as this approach was limited to dilute concentrations of only some cryoprotectants.

More recently, a broad range of experimental and computational methods have studied the physical properties of glycerol and its mixtures with water. While NMR,[12] infrared,[13] and Raman spectroscopy[14] have provided useful insights into the dynamic behavior of glycerol–water mixtures, it is perhaps surprising that the current view of its fundamental liquid structure is almost exclusively derived from computer simulations.[15−27] These investigations have been parametrized

Received: September 19, 2012
Revised: October 25, 2012
Published: October 26, 2012

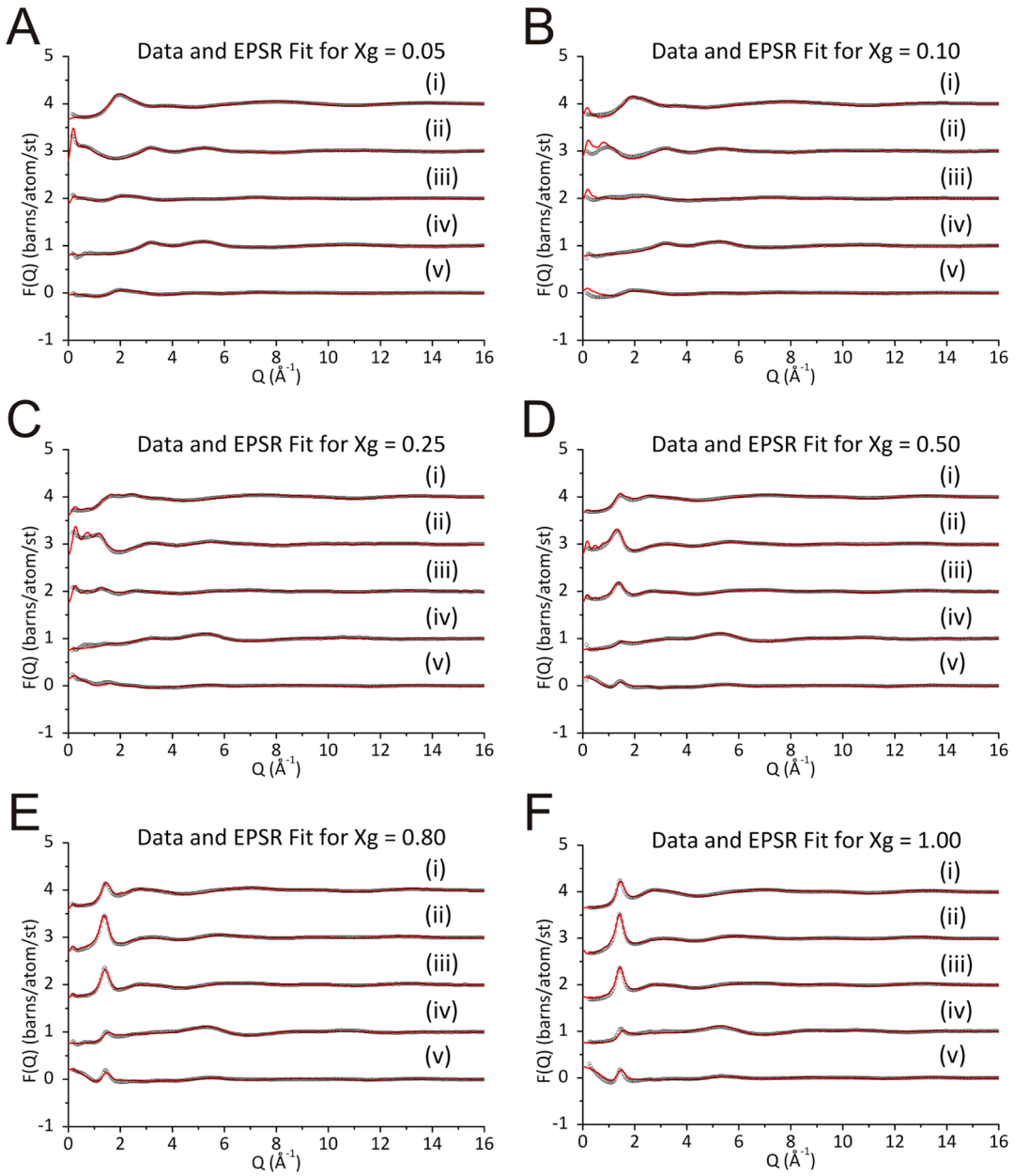

Figure 1. Experimental neutron diffraction data (black circles) and EPSR fits to the data (solid red lines) for each of the isotopic substitutions of glycerol–water solutions at concentration of mole fraction of glycerol (A) $x_g = 0.05$, (B) $x_g = 0.10$, (C) $x_g = 0.25$, (D) $x_g = 0.50$, (E) $x_g = 0.80$, and (F) $x_g = 1.00$. The data shown here confirm that the EPSR model is in good agreement with the experimental data.

to reproduce some macroscopic physical properties, such as the liquid's diffusion coefficient, but they are entirely dependent on the resulting interatomic and intermolecular force fields for the reproduction of structural parameters. Due to the absence of any parametrization to data which are directly related to atomic and molecular structure, conclusions derived from these models concerning local structure remain inconclusive. Despite this challenge, a recurring hypothesis in experimental and computational studies is that cryoprotectants act by modifying water structure.[19,28−30] However, this water modification view is at odds with a study using fundamental thermodynamic relations[31] which found no correlation between a cryoprotectants impact on water structure and its ability to stabilize a biological molecule. Instead, the study suggested that efforts to explain cryoprotectants actions should focus on other hypotheses, including those based on preferential interactions between water and the cryoprotectant. Indeed, an early study suggests that the behavior of aqueous glycerol is a result of differences in the hydrogen-bonding interactions between glycerol–glycerol, water–glycerol, and water–water interactions.[32] While conceptually attractive, there has been no direct structural evidence of this to date.

Kyrychenko et al.[22] completed molecular dynamics simulations to investigate the solubility behavior of cryoprotective solutes, such as glycerol, in pure water. This study suggested that while some cryoprotectants mix rapidly with water, glycerol molecules are nonideally mixed at the molecular level, and the mixing dynamics of the glycerol molecules is strongly dependent on the nature of the hydrophilic and hydrophobic interactions between the glycerol molecules.[22] In addition, other hypotheses rely on qualitative steric arguments based on molecular packing[33] and a combination of steric and

dx.doi.org/10.1021/jp3093034 | J. Phys. Chem. B 2012, 116, 13898−13904

interaction based mechanisms.[34,35] Clearly, a detailed structural study of aqueous glycerol across the full concentration range is required to directly test these hypotheses. The variability of results produced using computer simulations and the lack of experimental structural information mean that a more direct experimental probe of liquid structure is required to determine the influence of glycerol on the local and extended water structure. The present work directly addresses that need.

METHODS

Neutron diffraction experiments were completed at room temperature on the small angle neutron diffractometer for amorphous and liquid samples (SANDALS) time-of-flight diffractometer at the ISIS pulsed neutron facility within the Rutherford Appleton Laboratory, U.K. This instrument is optimized for the study of liquid samples containing hydrogen.[36−40] The experimental setup for the liquid sample measurements was similar to that employed in recent measurements of other solutions. The standard corrections and normalizations have been applied to the neutron data by means of the program Gudrun.[41] Deuteriated samples of water along with protiated and deuteriated samples of anhydrous glycerol were obtained from Sigma-Aldrich and used without additional purification. Experiments were completed across the full concentration range, including glycerol mole fraction x_g = 0.05, 0.10, 0.25, 0.50, 0.80, and 1.00. For each concentration a total of 5 samples were used, making use of relevant isotope substitution of the hydrogen (see SI Table S1 for a full list of samples).

The extraction of the real-space pair-distribution functions from the structure factors obtained from the neutron diffraction data needs their decomposition into a linear combination of partial structure factors. This task has been undertaken by means of data modeling based on the EPSR approach[42] which has previously been applied to glycerol mole fraction x_g = 0.05,[43] 0.80,[39] and 1.00.[44] In the present study, we structurally examine all six concentrations for the first time. This method is based on a classical NVT Monte Carlo simulation of the system under study which employs an iterative algorithm to achieve consistency between the experimental diffraction data and model functions derived from the statistically simulated system. The initial stage of the procedure consists of a thermalization of the simulation system by using a set of reference interparticle potentials. These initial potentials are modified by adding empirical terms in an iterative manner to minimize the residual function between the experimental and simulated structure factors. This approach has been employed for a broad range of aqueous solutions[45−47] and details of the procedure can be found elsewhere.[42,44] The SPC model was employed for water molecules.[48] Full details of the Lennard−Jones and charge parameters for water and glycerol molecules are given in the Supporting Information (SI Tables S2−4). Simulation boxes were built with the same molecular ratios as the experimental ratios (SI Table S5). In the simulation, we refer to 2 distinct atomic components in water and 6 distinct atomic components in glycerol molecules (SI Figure S1). In the water molecule, the oxygen atom is labeled OW, while the hydrogen atom is labeled HW. In glycerol, the carbon atoms are labeled CC and CG and refer to the central and distal carbon atoms respectively. The oxygen atoms are labeled OC and O corresponding to the oxygen atoms attached to the central and distal carbon atoms, respectively. The hydrogen atoms are labeled H and HG for the hydroxyl and methyl hydrogen atoms, respectively.

RESULTS AND DISCUSSION

At the molecular level, glycerol is a complex molecule to study, on account of its molecular flexibility, asymmetry, and ability to form hydrogen bonds.[44,49] An experimental approach is needed that can directly measure the hydrogen bonding ability of both glycerol and water across the concentration range. We have completed a detailed structural determination of glycerol−glycerol, glycerol−water, and water−water interactions. This has been completed across the full concentration range (glycerol mole fraction, x_g = 0.05, 0.10, 0.25, 0.50, 0.80, and 1.00). This thorough study was completed using neutron diffraction with hydrogen isotope labeling.[42] The diffraction data are interpreted by empirical potential structure refinement (EPSR). This approach provides detailed atomistic level structural information on glycerol and water in solution, crucial information for understanding their hydrogen bonding ability (SI Figure S1).

Figure 1 shows the neutron data together with the fitted data obtained by the EPSR model for all glycerol concentrations. The agreement of the simulated structure factors is good in all cases. From the EPSR molecular ensembles, we derive site−site radial distribution functions (RDFs), $g_{\alpha\beta}(r)$, which describe the relative density of one type of atom, β, as a function of distance, r, from another atom type α.

Figure 2 shows the most relevant pair distribution functions of the EPSR model that fit the experimental data taken from the EPSR analysis of neutron diffraction data for x_g = 0.50. These RDFs examine the hydrogen bonding between water−water, glycerol−glycerol, and glycerol−water molecules, as given by (A) $g_{OW\text{-}HW}(r)$, (B) $g_{O-H}(r)$, and (C) $g_{O\text{-}HW}(r)$ and $g_{OW\text{-}H}(r)$. For comparison, we show the relevant water−water and glycerol−glycerol distributions in the pure components (dashed lines). For all oxygen−hydrogen RDFs (Figure 2A−C) a first peak is observed at around 1.8 Å, a feature indicative of hydrogen bonding. For water−water interactions (Figure 2A), $g_{OW\text{-}HW}(r)$, the position of the first peak decreases marginally from 1.80 Å in pure water (dashed line) to 1.71 Å in x_g = 0.50 in x_g = 0.50 (solid line). Similarly for glycerol−glycerol interactions (Figure 2B), $g_{O-H}(r)$, the position of the first peak decreases marginally from 1.80 Å in pure glycerol (dashed line) to 1.74 Å in x_g = 0.50 (solid line). The peak positions do not change appreciably with glycerol concentration (SI Figure S2), suggesting that the local hydrogen bonding between glycerol−glycerol, glycerol−water, and water−water is not sensitive to glycerol content. These results challenge the hypothesis that the water structure is either enhanced or destroyed in aqueous glycerol. In order to develop a more quantitative understanding of the hydrogen bonding in glycerol−water solutions, we measured the hydrogen bonding ability of both the glycerol and water molecules as a function of glycerol concentration. This was compared to the hydrogen bonding of each molecule in the pure liquids. The degree of hydrogen bonding in the two liquids before mixing is estimated by calculating coordination numbers for pure glycerol and for pure water. We assume here that the oxygen−hydrogen coordination number up to the first minimum in the relevant oxygen−hydrogen RDF represents the number of hydrogen bonds associated with that atom pair. This analysis indicates that there are 5.71 hydrogen bonds per glycerol molecule in pure glycerol and 3.61 hydrogen bonds per water molecule in pure water.

For the glycerol−water mixtures, the number of hydrogen bonds was calculated using the coordination numbers around

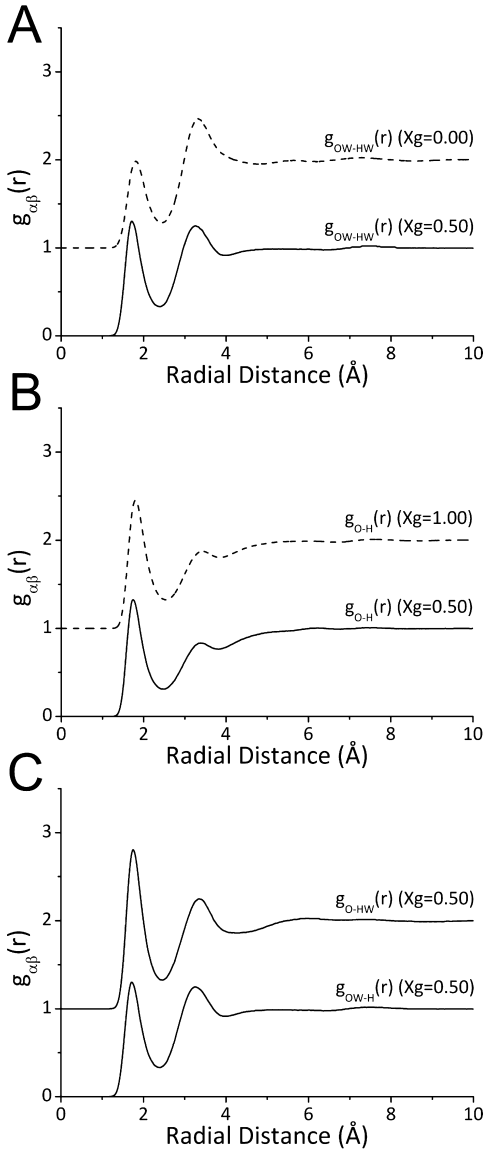

Figure 2. Radial distribution functions (RDFs) for the oxygen–hydrogen pairs that form hydrogen bonds in a glycerol–water solution (solid line) and in the pure liquids (dashed line). The signature of hydrogen bonding (a peak at around 1.8 Å) can be seen in each of the functions shown. The RDFs are taken from the EPSR analysis of neutron diffraction data for the x_g = 0.50 concentration. Similar functions have been produced for each of the concentrations studied (SI Figure S2).

relevant atoms for each corresponding oxygen–hydrogen RDF shown in Figure 2 and SI Figure S2. The number of hydrogen bonds formed by each molecule type is shown in Figure 3A. For each molecule, we distinguish between like–like or homointeractions (i.e., glycerol–glycerol or water–water) and unlike–unlike or heterointeractions (glycerol–water or water–glycerol). Two interesting features arise from these results. First, it can be seen that the total number of hydrogen bonds formed by each molecule type is relatively constant across the concentration range (Figure 3A). Second, the proportion of homo and hetero hydrogen bonding changes monotonically as a function of glycerol concentration (Figure 3B). Therefore, the hydrogen bonds between glycerol and water molecules created upon mixing compensate for the water–water and glycerol–glycerol hydrogen bonds lost upon mixing the pure liquids.

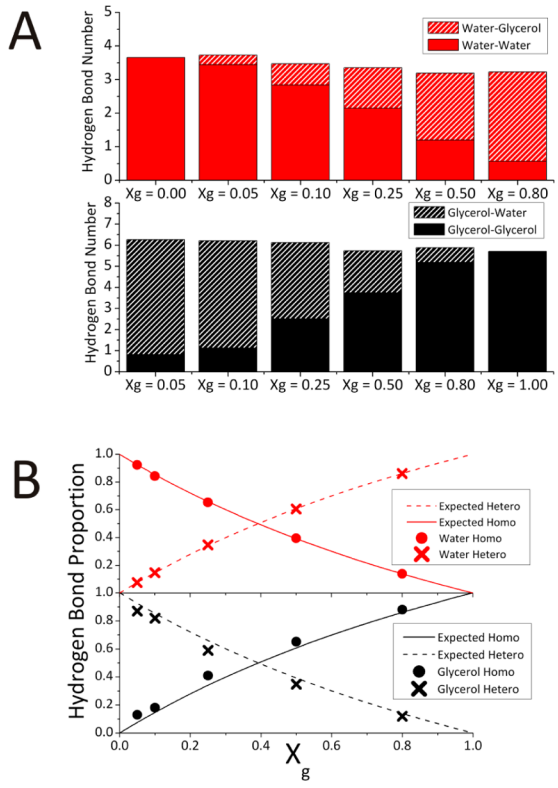

Figure 3. (a) Number of hydrogen bonds formed by each molecule type at each of the glycerol–water concentrations studied. Solid colors refer to homohydrogen bonds (water–water or glycerol–glycerol) and shaded colors refer to heterobonds (water–glycerol or glycerol–water). (b) Proportion of homo- (filled circles) and hetero- (crosses) hydrogen bonds for water (top) and glycerol (bottom) compared to a simple model based on the number of hydrogen bonds available. The calculation of the values for the model is described in the Supporting Information and solid and dashed lines refer to homo and hetero hydrogen bonding, respectively.

Interestingly, contrary to previous computational studies,[17,24] we find no evidence for intramolecular hydrogen bonds in glycerol. This lack of intramolecular hydrogen bonding may account for its tendency to hydrogen bond with other glycerol and water molecules.

To further examine the hydrogen bonding ability of glycerol and water we examined the distribution of water molecules and glycerol molecules in the system. The EPSR generated ensembles were interrogated to extract structural information on glycerol and water clusters in the solution. Representative snapshots of the glycerol–water solution are shown in Figure 4A where water molecules are represented by their oxygen atoms (red spheres) and glycerol molecules are represented by their carbon atoms in the backbone (black spheres).The snapshots show groups of water molecules hydrogen bonded together, forming clusters in the solution. Likewise, groups of glycerol molecules exist in glycerol-rich clusters. To quantitatively assess this microsegregation, we completed a full cluster analysis for both glycerol and water across the concentration range. The cluster analysis is derived from the simulation of the scattering data and provides further structural insight.[43,50] The cluster size distribution is the probability of finding a cluster of a particular size as a function of cluster size. The glycerol clusters and water clusters are defined by those molecules that participate in a continuous hydrogen bonded network. Using

dx.doi.org/10.1021/jp3093034 | J. Phys. Chem. B 2012, 116, 13898–13904

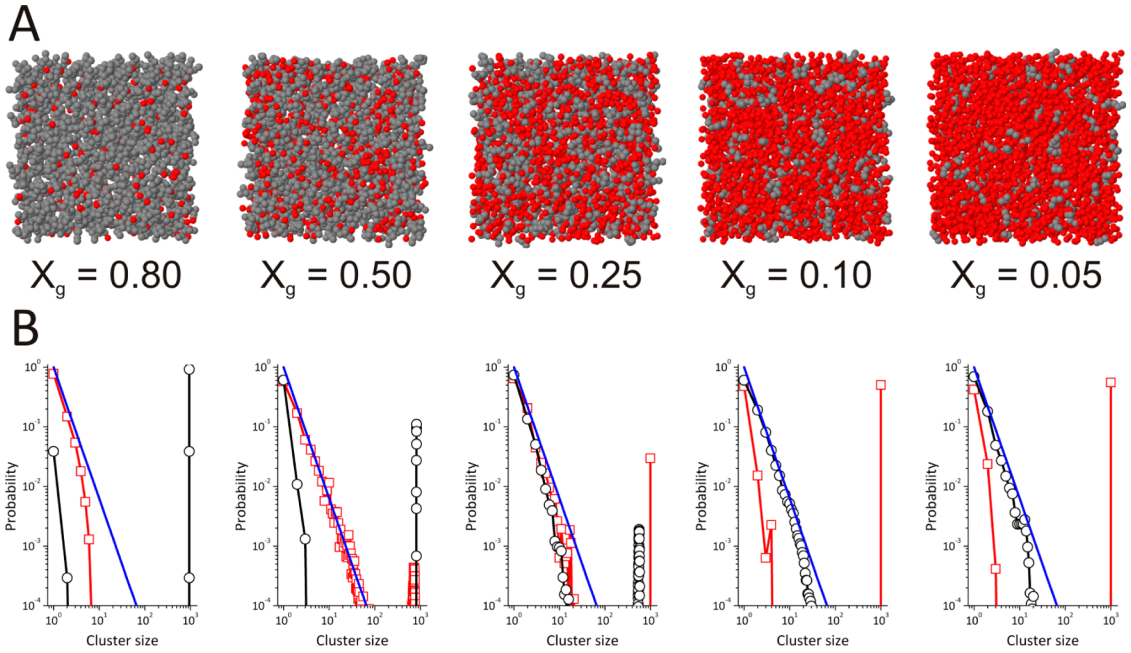

Figure 4. (a) Snapshots of the EPSR simulation box showing only carbon (black) and water-oxygen atoms (red) at each of the glycerol–water concentrations studied. The molecular scale segregation is shown by clusters of glycerol (black) and water (red) molecules. (b) Cluster size distributions for glycerol (black circles) and water (red squares) molecules at each of the glycerol–water concentrations studied along with the 3D percolation threshold[51] (blue line). These data show that percolating water clusters appear (shown by red data points to the right of the blue line) in all concentrations apart from $x_g = 0.80$. Similarly, percolating glycerol clusters are found at all concentrations of $x_g \geq 0.25$ (shown by black data points to the right of the blue line). Therefore, there is a bipercolating mixture at $0.25 < x_g < 0.50$ (both red and black data points to the right of the blue line).

the structural information from the relevant RDFs, two glycerol molecules are hydrogen-bonded if the interoxygen contact distance is less than the radial distance of the first minimum of the relevant RDFs; $g_{O-O}(r)$, $g_{O\text{-}OC}(r)$, and $g_{OC\text{-}OC}(r)$. Two water molecules are hydrogen-bonded if the interoxygen contact distance is less than the radial distance of the first minimum of the $g_{OW\text{-}OW}(r)$.

Figure 4B shows the number of clusters containing i glycerol/water molecules as a fraction of the total number of clusters $M(i)/M$ [where $M = \Sigma i\ M\ (i)$] against cluster size i. Here, a percolating cluster is defined as having a distribution that crosses the random 3-dimensional percolation threshold[51] given by the power law $N = S^{-2.2}$. Here N is the cluster proportion and S is the size of the cluster. The data show that glycerol and water microsegregates to form water-rich clusters and glycerol rich-clusters. These regions exist as hydrogen-bonded strings and clusters which differ in size across the concentration range. In the concentrated glycerol region, the majority (56%) of water molecules exist as single monomers. This preference for isolated water molecules results in a well-mixed solution with optimal glycerol–water hydrogen bonding. In the dilute glycerol region, there is a prevalence of isolated glycerol molecules (40%), again resulting in a well-mixed solution with glycerol–water hydrogen bond interactions being favorable. We find that large percolating water clusters exist at glycerol mole fractions below $x_g = 0.50$, while large percolating glycerol clusters exist at glycerol mole fractions above $x_g = 0.25$. Thus, at a concentration of $0.25 \leq x_g \leq 0.50$, a solution exists which is composed of a bipercolating mixture with both glycerol hydrogen bonding clusters and water hydrogen bonded clusters spanning the entire system. We also examine the fraction of molecules in the interface between glycerol clusters and water clusters. The interface is defined by hydrogen bond interactions between glycerol and water and is calculated using the relevant radial distribution functions. Interestingly, we find a maximum in the fraction of molecules in the interface at a mole fraction of $x_g = 0.50$ (SI Figure S3). Therefore, at this concentration, the solution is both a bipercolating liquid mixture and maximizing its heterohydrogen bond interactions. This suggests a delicate balance between hetero and homo interactions in this system.

By considering the hydrogen bonding of each molecule as well as the microsegregation in the system, a detailed picture emerges of the hydrogen bonding ability of the glycerol–water mixture. At all concentrations studied, water maintains its hydrogen bond ability, forming around 4 hydrogen bonds per molecule (Figure 3A). This is achieved by a balance between water–water and glycerol–water hydrogen bonds. At the same time, both water and glycerol maintain a hydrogen bonded network, forming clusters which differ in size and dimensions across the concentration range (Figure 4). The proportion of molecules found in percolating clusters for glycerol and water is shown in Figure 5. At all concentrations, glycerol effectively gets in the way of water clusters. This can be seen in the dilute glycerol region, where isolated glycerol molecules exist, maximizing glycerol–water interactions, while in the concentrated glycerol region isolated water molecules exist. The gray region highlights the concentration range over which the mixture is bipercolating. Within this concentration range, the hydrogen bonding ability of glycerol and water allow both species to exist as percolating networks in the system.

CONCLUSIONS

The structure of glycerol–water solutions across the concentration range have been experimentally determined by the combined use of neutron diffraction techniques and an

dx.doi.org/10.1021/jp3093034 | J. Phys. Chem. B 2012, 116, 13898–13904

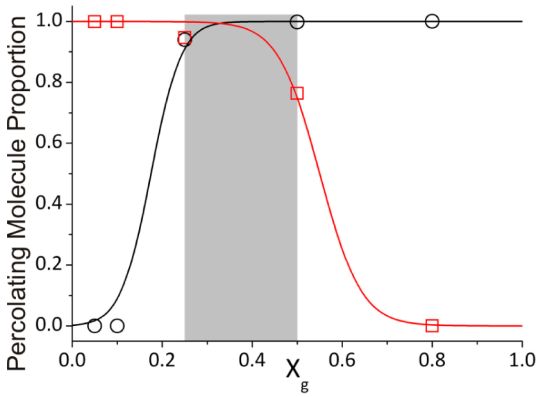

Figure 5. Proportion of molecules found in percolating clusters for glycerol (black circles) and water (red squares). The gray region shows the concentration range that the mixture is bipercolating (both water and glycerol form percolating networks) the solid lines shown are sigmoidal functions to guide the eye.

atomistic representation of the system based on a designed reverse Monte Carlo procedure, the EPSR method. This approach, specifically sensitive to the hydrogen atoms in the system, has been key to achieving unambiguous experimental insight into the hydrogen bonding ability in glycerol–water solutions. Fundamental insights have been achieved from the analysis of the present data. Contrary to previous expectations, we show that the hydrogen bonding ability of water is not diminished in the presence of glycerol. Instead, we show that the total number of hydrogen bonds formed by water is relatively constant across the concentration range. We show that the proportion of homo- and hetero-hydrogen bonding changes monotonically as a function of glycerol concentration (Figure 3B), demonstrating that the hydrogen bonds between glycerol and water molecules created upon mixing compensate for the water–water hydrogen bonds lost. This result, obtained from experimental data, directly challenges the hypothesis that water structure is either enhanced or destroyed in aqueous glycerol. The water structuring hypothesis has also been challenged in a neutron diffraction study on two different concentrations of aqueous trehalose.[52] This study found that trehalose solvation induces very minor modification of water structure, with the average number of bonds per water molecule almost unchanged. This is in agreement with an extensive molecular dynamics simulation study of six different polyol–water solutions, including glycerol, which found that hydrogen bonds lost between water molecules are replaced by bonds formed with polyols.[26] However, as is the case for glycerol–water solutions, other studies have suggested that trehalose acts to disturb the hydrogen bonded network of water.[53−55]

We quantitatively examine the hydrogen bond networks in glycerol–water solutions across the concentration range. The data show that glycerol and water microsegregates to form hydrogen bonded strings and clusters of water-rich regions and glycerol rich-regions. These clusters differ in size across the concentration range, from small clusters of size two to clusters which account for all of the molecules in the system. These percolating clusters exist for glycerol at high glycerol mole fraction ($x_g \geq 0.25$) and for water at low glycerol mole fraction ($x_g \leq 0.50$). Interestingly, we show there is a concentration range ($0.25 \leq x_g \leq 0.50$) where glycerol–water solutions exist as a bipercolating, hydrogen-bonded network, composed of a percolating glycerol cluster and a percolating water cluster. In addition, the fraction of all molecules in the interface between glycerol clusters and water clusters reaches a maximum at $x_g = 0.50$. This suggests a delicate balance between hetero and homo interactions in this system around this concentration. Interestingly, the mole fraction range over which simultaneous two-component percolation occurs coincides with the concentration range at which many thermodynamic properties show extremes.[28]

Microsegregation and clustering have been observed in other cryoprotectant-water mixtures. Pronounced microheterogeneity in a concentrated sorbitol–water mixture (mole fraction sorbitol $x = 0.19$, 70% weight sorbitol) was measured using wide and small angle neutron scattering.[56] In this system, water molecules formed clusters surrounded by sorbitol molecules. Computational studies of carbohydrates such as fructose,[57] sucrose[58,54] and trehalose,[54,59] and polyols such as glycerol[26] have also identified self-association leading to concentration-dependent clustering. Efforts have been made to link such cryoprotectant association to solution properties, for example osmotic pressure.[26] This offers a promising route to understand and predict the solution properties and cryoprotective action of molecules for biopreservation and stabilization. The current study on aqueous glycerol across the whole concentration range provides experimental, structural data which can now be exploited to develop such predictive tools.

On the basis of our data and simulations, we propose a coherent view of the cryoprotectant ability of glycerol–water solutions. At its heart, is the fact that glycerol readily substitutes for water in forming hydrogen bonds. As a result, at different concentrations, the total number of hydrogen bonds per water molecule remains close to 4. At the same time, at all concentrations, glycerol segregates the water into clusters. Even where these water clusters are percolating, the combination of maintaining hydrogen bond number while imposing water segregation, would prevent the formation of ice and the cell damaging volume expansion that would accompany that formation. This must call the attention of the scientific community to the role of hydrogen bonding connectivity rather than water structuring/destructuring effects in these important cryoprotective systems.

■ ASSOCIATED CONTENT

Supporting Information

Tables with full list of samples for all concentrations and Lennard–Jones and charge parameters employed for the reference intermolecular potentials in the EPSR method are included. This material is available free of charge via the Internet at http://pubs.acs.org.

■ AUTHOR INFORMATION

Corresponding Author

*E-mail: L.Dougan@leeds.ac.uk.

Notes

The authors declare no competing financial interest.

■ ACKNOWLEDGMENTS

This work was supported by the Engineering Physical Science Research Council, UK through grant EP/H020616 to Lorna Dougan and through a DTA studentship to James Towey. Experiments at the ISIS Pulsed Neutron and Muon Source were supported by a beam time allocation from the Science and Technology Facilities Council. We are grateful to Dr. Daniel

Bowron, Dr. Silvia Imberti, and Dr. Rowan Hargreaves at the ISIS Facility, RAL, U.K. for their support. We thank Prof. Stephen Evans and members of the Dougan group at University of Leeds for useful discussions.

REFERENCES

(1) Polge, C.; Smith, A. U.; Parkes, A. S. *Nature* **1949**, *164*, 666−666.
(2) Lovelock, J. E. *Biochim. Biophys. Acta* **1953**, *11*, 28−36.
(3) Mazur, P. *Science* **1970**, *168*, 939−949.
(4) Fuller, B. J. *Cryoletters* **2004**, *25*, 375−388.
(5) Bernemann, I.; Hofmann, N.; Spindler, R.; Szentivanyi, A.; Glasmacher, B. *Cryoletters* **2008**, *29*, 83−83.
(6) Fuller, B.; Paynter, S. *Reprod. Biomed. Online* **2004**, *9*, 680−691.
(7) Lovelock, J. E.; Polge, C. *Biochem. J.* **1954**, *58*, 618−622.
(8) Muldrew, K.; Mcgann, L. E. *Biophys. J.* **1990**, *57*, 525−532.
(9) Lobo, R. A. *N. Engl. J. Med.* **2005**, *353*, 64−73.
(10) Karow, A. M.; Webb, W. R. *Cryobiology* **1965**, *1*, 270−273.
(11) Nash, T. In *Cryobiology*; Academic Press: New York, 1966.
(12) Doss, A.; Paluch, M.; Sillescu, H.; Hinze, G. *Phys. Rev. Lett.* **2002**, *88*, 095701−095705.
(13) Vanderkooi, J. M.; Dashnau, J. L.; Zelent, B. *Biochim. Biophys. Acta-Proteins Proteom.* **2005**, *1749*, 214−233.
(14) Mudalige, A.; Pemberton, J. E. *Vib. Spectrosc.* **2007**, *45*, 27−35.
(15) Blieck, J.; Affouard, F.; Bordat, P.; Lerbret, A.; Descamps, M. *Chem. Phys.* **2005**, *317*, 253−257.
(16) Callam, C. S.; Singer, S. J.; Lowary, T. L.; Hadad, C. M. *J. Am. Chem. Soc.* **2001**, *123*, 11743−11754.
(17) Chelli, R.; Procacci, P.; Cardini, G.; Califano, S. *Phys. Chem. Chem. Phys.* **1999**, *1*, 879−885.
(18) Chelli, R.; Procacci, P.; Cardini, G.; Della Valle, R. G.; Califano, S. *Phys. Chem. Chem. Phys.* **1999**, *1*, 871−877.
(19) Chen, C.; Li, W. Z.; Song, Y. C.; Yang, J. *J. Mol. Liq.* **2009**, *146*, 23−28.
(20) Dashnau, J. L.; Nucci, N. V.; Sharp, K. A.; Vanderkooi, J. M. *J. Phys. Chem. B* **2006**, *110*, 13670−13677.
(21) Guardia, E.; Marti, J.; Padro, J. A.; Saiz, L.; Komolkin, A. V. *J. Mol. Liq.* **2002**, *96*−*7*, 3−17.
(22) Kyrychenko, A.; Dyubko, T. S. *Biophys. Chem.* **2008**, *136*, 23−31.
(23) Padro, J. A.; Saiz, L.; Guardia, E. *J. Mol. Struct.* **1997**, *416*, 243−248.
(24) Root, L. J.; Berne, B. J. *J. Chem. Phys.* **1997**, *107*, 4350−4357.
(25) Yongye, A. B.; Foley, B. L.; Woods, R. J. *J. Phys. Chem. A* **2008**, *112*, 2634−2639.
(26) Politi, R.; Sapir, L.; Harries, D. *J. Phys. Chem. A* **2009**, *113*, 7548−7555.
(27) Weng, L. D.; Chen, C.; Zuo, J. G.; Li, W. Z. *J. Phys. Chem. A* **2011**, *115*, 4729−4737.
(28) Marcus, Y. *Phys. Chem. Chem. Phys.* **2000**, *2*, 4891−4896.
(29) Schiffer, C. A.; Dotsch, V. *Curr. Opin. Biotechnol.* **1996**, *7*, 428−432.
(30) Branca, C.; Magazu', V.; Maisano, G.; Migliardo, F.; Soper, A. K. *Appl. Phys. A-Mater. Sci. Proc.* **2002**, *74*, S450−S451.
(31) Pielak, G. J.; Batchelor, J. D.; Olteanu, A.; Tripathy, A. *J. Am. Chem. Soc.* **2004**, *126*, 1958−1961.
(32) Fort, R. J.; Moore, W. R. *Trans. Faraday Soc.* **1965**, *61*, 2102−2111.
(33) Battino, R. *Chem. Rev.* **1971**, *71*, 5−45.
(34) Letcher, T. M.; Bricknell, B. C. *J. Chem. Eng. Data* **1996**, *41*, 639−643.
(35) Morrone, S. R.; Francesconi, A. Z. *Fluid Phase Equilib.* **2012**, *313*, 52−59.
(36) Bowron, D. T.; Finney, J. L.; Soper, A. K. *J. Phys. Chem. B* **1998**, *102*, 3551−3563.
(37) Imberti, S.; Bowron, D. T. *J. Phys.: Condens. Matter* **2010**, *22*, 404212−404226.
(38) McLain, S. E.; Soper, A. K.; Terry, A. E.; Watts, A. *J. Phys. Chem. B* **2007**, *111*, 4568−4580.
(39) Towey, J. J.; Soper, A. K.; Dougan, L. *J. Phys. Chem. B* **2011**, *115*, 7799−7807.
(40) Mancinelli, R.; Botti, A.; Bruni, F.; Ricci, M. A.; Soper, A. K. *J. Phys. Chem. B* **2007**, *111*, 13570−13577.
(41) Soper, A. K.; Howells, S.; Hannon, A. C. *ATLAS—Analysis of Time-of-Flight Diffraction Data from Liquid and Amorphous Samples* **1999**.
(42) Soper, A. K. *Phys. Rev. B* **2005**, *72*, 104204−104216.
(43) Towey, J. J.; Dougan, L. *J. Phys. Chem. B* **2012**, *116*, 1633−1641.
(44) Towey, J. J.; Soper, A. K.; Dougan, L. *Phys. Chem. Chem. Phys.* **2011**, *12*, 9397−9046.
(45) Bowron, D. T.; Beret, E. C.; Martin-Zamora, E.; Soper, A. K.; Marcos, E. S. *J. Am. Chem. Soc.* **2012**, *134*, 962−967.
(46) Hargreaves, R.; Bowron, D. T.; Edler, K. *J. Am. Chem. Soc.* **2011**, *133*, 16524−16536.
(47) Dixit, S.; Crain, J.; Poon, W. C. K.; Finney, J. L.; Soper, A. K. *Nature* **2002**, *416*, 829−832.
(48) Robinson, G. W.; Zhu, S. B.; Singh, S.; Evans, M. W. *Water in Biology, Chemistry and Physics: Experimental Overviews and Computational Methodologies*; World Scientific: Singaore, 1996.
(49) Bastiansen, O. *Acta Chem. Scand.* **1949**, *3*, 415−421.
(50) Dougan, L.; Bates, S. P.; Hargreaves, R.; Fox, J. P.; Crain, J.; Finney, J. L.; Reat, V.; Soper, A. K. *J. Chem. Phys.* **2004**, *121*, 6456−6462.
(51) Jan, N. *Physica A* **1999**, *266*, 72−75.
(52) Pagnotta, S. E.; McLain, S. E.; Soper, A. K.; Bruni, F.; Ricci, M. A. *J. Phys. Chem. B* **2010**, *114*, 4904−4908.
(53) Lerbret, A.; Bordat, P.; Affouard, F.; Guinet, Y.; Hedoux, A.; Paccou, L.; Prevost, D.; Descamps, M. *Carbohydr. Res.* **2005**, *340*, 881−887.
(54) Lerbret, A.; Bordat, P.; Affouard, F.; Descamps, M.; Migliardo, F. *J. Phys. Chem. B* **2005**, *109*, 11046−11057.
(55) Branca, C.; Magazu, S.; Maisano, G.; Migliardo, P. *J. Chem. Phys.* **1999**, *111*, 281−287.
(56) Chou, S. G.; Soper, A. K.; Khodadadi, S.; Curtis, J. E.; Krueger, S.; Cicerone, M. T.; Fitch, A. N.; Shalaev, E. Y. *J. Phys. Chem. B* **2012**, *116*, 4439−4447.
(57) Sonoda, M. T.; Skaf, M. S. *J. Phys. Chem. B* **2007**, *111*, 11948−11956.
(58) Molinero, V.; Cagin, T.; Goddard, W. A. *Chem. Phys. Lett.* **2003**, *377*, 469−474.
(59) Sapir, L.; Harries, D. *J. Phys. Chem. B* **2011**, *115*, 624−634.